Strain-Dependent Photoluminescence Line Shifts of the TS Color Center in 4H-SiC

J.A.F. Lehmeyer[1,a*], A.D. Fuchs[1,b], T. Bornträger[1,c], M.A. Popp[2,d],
H.B. Weber[2,e], and M. Krieger[1,f],

Lehrstuhl für Angewandte Physik, Department Physik, Friedrich-Alexander-Universität
Erlangen-Nürnberg (FAU),
Staudststr. 7, 91058 Erlangen, Germany

[a]johannes.lehmeyer@fau.de, [b]alexander.d.fuchs@fau.de, [c]titus.borntraeger@fau.de,
[d]matthias.popp@fau.de, [e]heiko.weber@fau.de, [f]michael.krieger@fau.de

Abstract. We present a detailed study of the behavior of the photoluminescence (PL) of the TS color center in 4H-SiC under controlled mechanical strain. We have investigated the TS1 line under varying strain, including its reaction to compression and tension. We use emission polarization measurements to gain access to the orientation of the underlying defects. We put our results in context with previous findings and find good agreement, corroborating the proposed microscopic model.

Introduction

In recent years color centers in SiC have gained increasing attention due to their unique properties. With their character as single photon sources, they are an excellent basis for on-chip photonic quantum technologies [1]. Even in comparison to the highly studied nitrogen-vacancy center in diamond, color centers in SiC show favorable properties [2]. With 4H-SiC as a mature semiconductor for power electronics, it furthermore benefits from advanced processing technologies [3].

Since a perfect crystalline environment is preferable for quantum technology, a defect that survives high temperature annealing is advantageous. One such candidate is the aptly named temperature stable (TS) defect, which is virtually the only defect present after annealing above 1200°C [4]. The TS defect may be produced in various ways including proton and laser irradiation [4, 5]. In previous work, it was shown that the TS defect is strongly influenced by mechanical strain [6].

In the previous work, however, the strain was introduced via a scratch in the surface. Now we aim for a measurement with more well-defined strain. Such a measurement should help one understand how exactly the TS defect reacts to strain and also give insight of its microscopic description.

Experimental Methods

Sample Processing.

We cut our samples from a commercial high-purity semi-insulating (HPSI) 4H–SiC on-axis wafer into sticks of 8 by 0.5 mm with a thickness of 0.5 mm. These narrow samples allow us to approximate the deformation to be mainly one-dimensional. The samples are cut in two different directions, either with the long side of the sample along the $(11\bar{2}0)$ direction or along the $(1\bar{1}00)$ direction.

The samples are irradiated with protons of an energy of 350 keV and a dose of 10^{15} cm^{-2}. Using TRIM calculations [7], the damage is at its maximum at 2.4 μm below the surface and can be neglected after 2.6 μm. The vacancies introduced via the irradiation are converted to the TS color center by annealing at 1200°C under Ar-atmosphere [6].

All measurements in this work are performed from the Si-face of the crystal.

Measurement Setup.

We use a custom-built confocal microscope for the measurements. A 532 nm laser was used for the excitation. Stress is induced by an improved version of the squeezable nanojunction presented in [8].
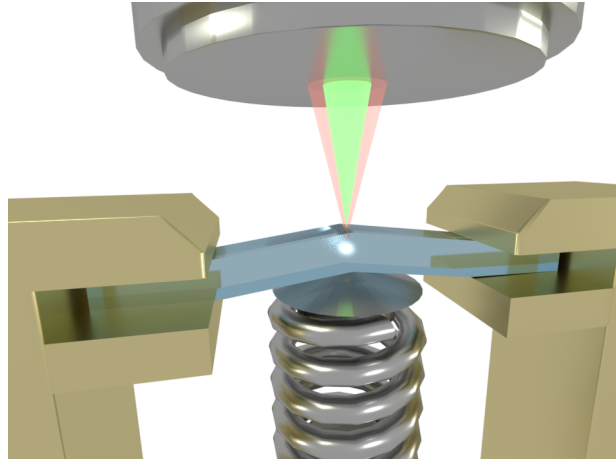
Fig. 1: Artist's view of the squeezable nanojunction [8] adjusted for the bending of SiC-sticks. The sample is fixed on both ends and a mandrel presses upwards against the center of the stick, while the sample can be investigated with PL measurements.

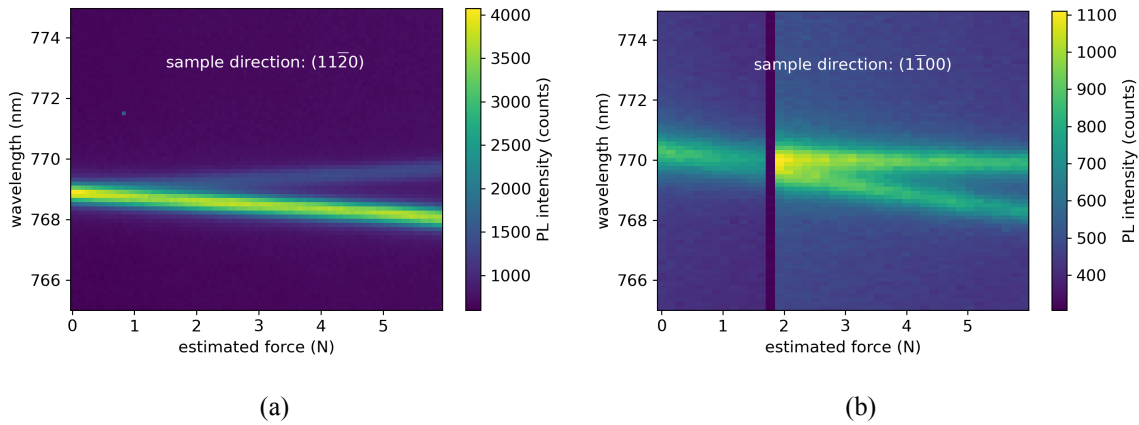(a)   (b)

Fig. 2: Spectra of the TS1 line for increasing force for (a) a sample in $(11\bar{2}0)$ direction and (b) a sample in $(1\bar{1}00)$ direction. In both samples the splitting grows with the force. The splitting is different for each sample, as the resulting strain is along the same crystal-axis as the sample.

An artist's impression of the setup is shown in Fig. 1. With the setup, the sample can be fixed from the top and a mandrel can be pressed against the sample from the bottom. By adjusting the force, we can bend the SiC-sticks in a controlled manner. Calibration of the force was performed in a separate experiment using a force sensor. During the measurement, the sample is located inside a cryostat and cooled to ~100 K. Since the TS2 and TS3 lines behave in the same way as the TS1 line under strain [6], this work focuses on the latter due to its stronger PL intensity.

Photoluminescence of the TS Defect Under Controlled Strain

Splitting under varying force

Fig. 2 shows the spectra of the TS1 line over increasing force for a sample cut in $(11\bar{2}0)$ direction and a sample cut in $(1\bar{1}00)$ direction. The increased strain splits the lines further apart in both samples. The splitting differs between the samples, as the direction of the strain is along the crystal-axis along which the sample was cut. Both samples emit one weaker and one stronger line. While the weaker line is redshifted for the $(11\bar{2}0)$-sample, it is blueshifted for the $(1\bar{1}00)$-sample.

Splitting at different positions on the sample

The spectra of a scan along the $(11\bar{2}0)$-sample are shown in Fig. 3, together with schematics of the

position in the setup. The splitting is strongest right above the mandrel. Going towards the edge, the lines converge at first and then split again, close to the mounting. At this position, however, the weaker line is blue shifted, in contrast to being red shifted at the mandrel. This implies that for one defect configuration, tension increases the energy of the transition while compression decreases it. For the configuration responsible for the other PL-line, it is reversed.
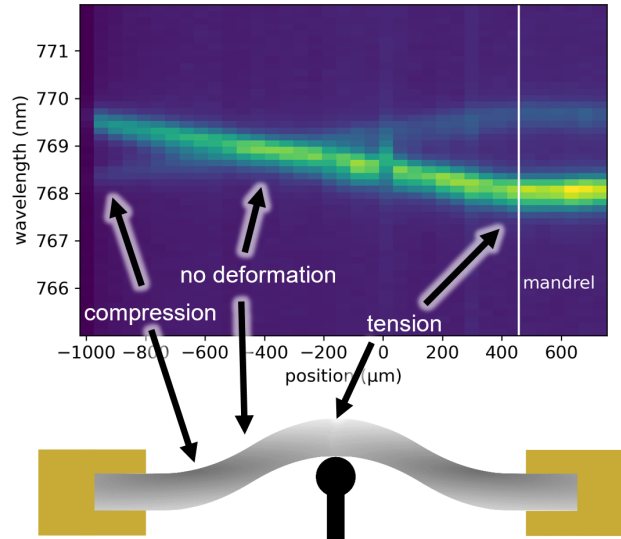

Fig. 3: Spectra of the TS1 line when scanning along the $(11\bar{2}0)$-sample under applied force. The schematics at the bottom give a reference to the position. The weaker line is red-shifted at the mandrel, but blue-shifted close to the mounting of the sample. In between, where almost no strain exists, the lines converge back into one single line.

Polarization of the split lines

To get a better understanding of the nature of the split TS1 lines, emission polarization measurements were performed for both samples at the mandrel-position. The results are depicted in Fig. 4(a) and 4(b). The peak with lower PL intensity is polarized perpendicular to the $(11\bar{2}0)$-axis, thus along the $(1\bar{1}00)$ direction. The polarization of the second peak is less pronounced, yet clearly apparent along $(11\bar{2}0)$. Fits to the polarization characteristics were performed with a single cosine for the pronounced peak and two 120°-shifted cosines for the other peak as in [6]:

$$f(x) \;=\; \frac{1}{2}(\cos(x + \phi) + 1) \tag{1}$$

$$g(x) \;=\; \frac{1}{2}(f(x + 120°) + f(x - 120°)). \tag{2}$$

The fits result in $\phi_{(11\bar{2}0),\text{red}} = 89.4°$, $\phi_{(11\bar{2}0),\text{blue}} = 90.3°$, $\phi_{(1\bar{1}00),\text{red}} = 86.0°$ and $\phi_{(1\bar{1}00),\text{blue}} = 86.6°$, which corroborates the aforementioned directions of the polarization. The shift of about $4°$ for the $(1\bar{1}00)$-sample may be due to a slightly misaligned sample in the setup.

Microscopic Model of the TS Color center

Overall, the measurements agree with the proposed model from [6]: The TS color center has three distinct orientations in the basal next-nearest neighbor (NNN) directions. Each defect-complex consists of three points in the crystal lattice. A highly probable candidate for the identification of the TS color center is the carbon di-vacancy-antisite complex $(V_C C_{Si} V_C)$ [9]. Fig. 4(c) shows the schematics of such a complex with respect to the applied strain. For both sample-types, two of the orientations have the same symmetry regarding the strain. Hence, these two orientations are seen as a single, overlapping peak, leaving only two peaks to observe instead of three. The good agreement of measurement
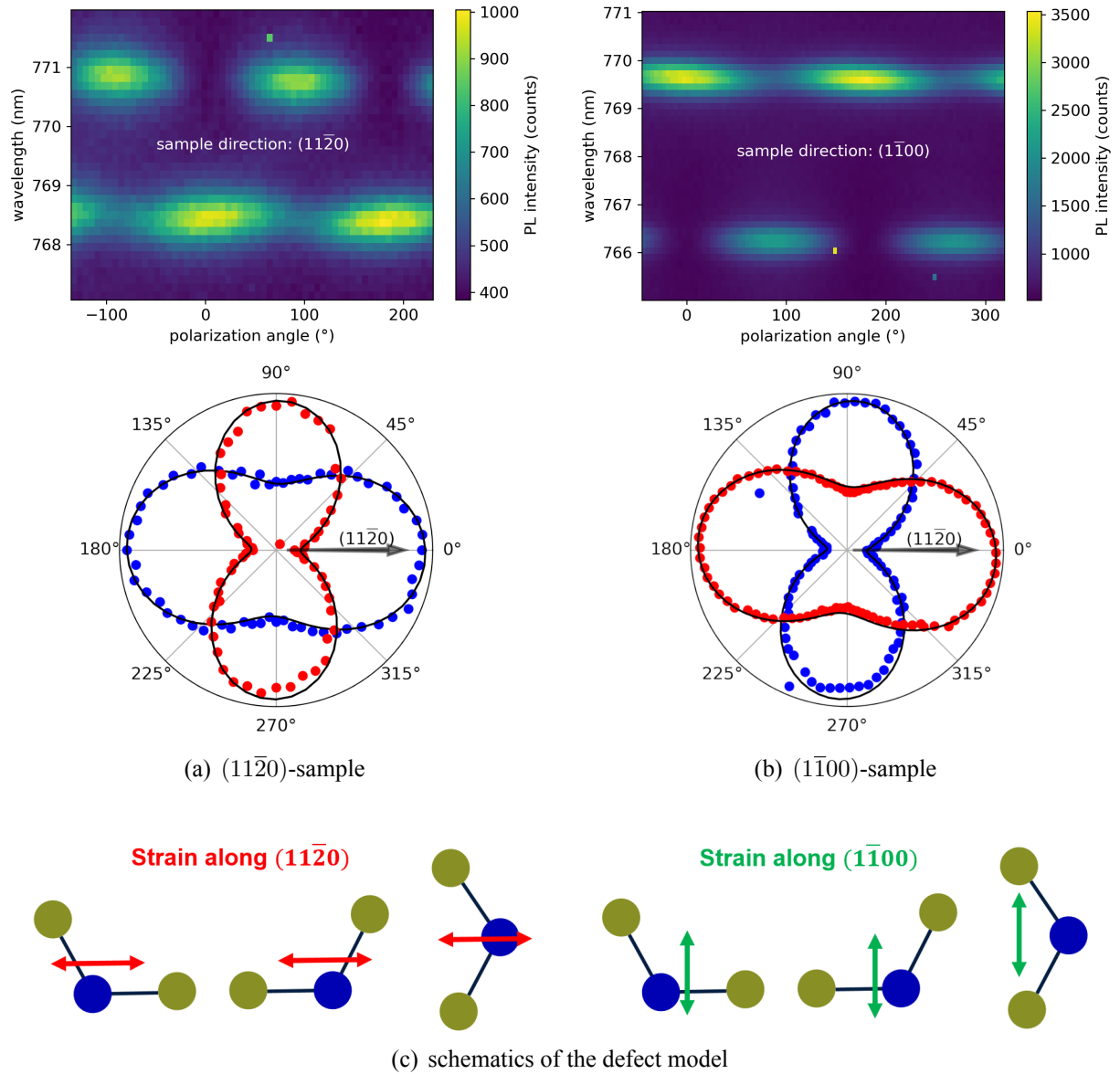
(a) $(11\bar{2}0)$-sample

(b) $(1\bar{1}00)$-sample

(c) schematics of the defect model

Fig. 4: Emission polarization measurements of the $(11\bar{2}0)$-sample (a) and the $(1\bar{1}00)$-sample (b) at the mandrel. The polar plots show the normalized intensity of each peak. Hereby, the peak with the shorter wavelength corresponds to the blue dots, the peak with the longer wavelength to the red dots. The angles were chosen so that the $(11\bar{2}0)$ axis corresponds to $0°$. The black lines are fits with Eq. 1 to the peak with more pronounced polarization and Eq. 2 to the other one. (c) depicts the schematics of our current microscopic model of the TS defect ($V_C C_{Si} V_C$ [9], V_C in green, C_{Si} in blue) along with the direction of the strain. For both directions of strain, two orientations of the defect complex have the same symmetry with respect to the strain, resulting in the peak with less distinct polarization.

data and double-cosine fit also reinforces this proposition and is further strengthened by the good fit of the single cosine for the other peak.

There are six equivalent defect orientations. For one given strain-vector, symmetry reduction leaves two equivalent sites that show the same response. Only one of each is displayed in Fig 4(c). Consequently there are only two peaks to observe. Upon further symmetry reduction, four peaks are observed [6], like in Stark-effect measurements which are sensitive to the polarity of the electric field.

Summary

In conclusion, we investigated the splitting of the TS photoluminescence lines under controlled mechanical strain. We showed that the lines split further with increased strain. Additionally, we could demonstrate that the lines react to different strain, namely tension and compression, in opposing ways. Emission polarization measurements allowed to distinguish the underlying defect-orientation for the split lines. Although additional work is required to completely understand all aspects of the TS color center, our detailed study of its behavior under mechanical strain is in agreement with previous findings.

References

[1] M.D. Eisaman, J.F.A. Migdall, S.V. Polyakov, Rev. Sci. Instrum. 82, 071101 (2011).

[2] R. Nagy, M. Niethammer, M. Widmann, Y.-C. Chen, P. Udvarhelyi, C. Bonato, J.U. Hassan, R. Karhu, I.G. Ivanov, N.T. Son, J.R. Maze, T. Oshima, Ö.O. Soykal, A. Gali, S.-Y. Lee, F. Kaiser, J. Wrachtrup, Nat Commun 10, 1954 (2019).

[3] T. Kimoto and J.A. Cooper, Fundamentals of Silicon Carbide Technology: Growth, Characterization, Devices and Applications (Wiley, Singapore, 2014).

[4] M. Rühl, C. Ott, S. Götzinger, M. Krieger, H.B. Weber, Appl. Phys. Lett. 113, 122102 (2018).

[5] S. Castelletto, J. Maksimovic, T. Katkus, T. Ohshima, B.C. Johnson and S. Juodkazis, Nanomaterials 11, 72 (2021).

[6] M. Rühl, J. Lehmeyer, R. Nagy, M. Weißer, M. Bockstedte, M. Krieger, H.B. Weber, New J. Phys. 23, 073002 (2021).

[7] J.F. Ziegler, J.P. Biersack, U. Littmark, The stopping and range of ions in solids (Pergamon, New York 1985).

[8] M.A. Popp, M. Kohring, A. Fuchs, S. Korn, N. Moses Badlyan, J. Maultzsch, H.B. Weber, 2D Mater. 8, 045034 (2021).

[9] M. Schober, N. Jungwirth, T. Kobayashi, J.A.F. Lehmeyer, M. Krieger, H.B. Weber, and M. Bockstedte, The optical properties of the carbon di-vacancy-antisite complex in the light of the TS photoluminescence center, Material Science Forum, Conference Proceedings ICSCRM 2022